Chemical Science

ROYAL SOCIETY OF CHEMISTRY

EDGE ARTICLE

View Article Online
View Journal | View Issue

Cite this: *Chem. Sci.*, 2023, **14**, 12339

All publication charges for this article have been paid for by the Royal Society of Chemistry

Received 17th May 2023
Accepted 9th October 2023

DOI: 10.1039/d3sc02515b

rsc.li/chemical-science

Metal–organic framework-derived CoN_x nanoparticles on N-doped carbon for selective *N*-alkylation of aniline†

Ved Vyas, Priyanka Maurya and Arindam Indra *

N-alkylation of anilines by alcohols can be used as an efficient strategy to synthesise a wide range of secondary amines. In this respect, a hydrogen borrowing methodology has been explored using precious metal-based catalysts. However, the utilisation of cheap and readily available transition metal based catalysts is required for large-scale applications. In this work, we have reported metal–organic framework-derived CoN_x@NC catalysts for the selective *N*-alkylation of anilines with different types of alcohols. The Co–N coordination in CoN_x@NC was found to be extremely important to improve the conversion efficiency and yield of the product. As a result, CoN_x@NC produced 99% yield of the desired amines, which is far better than that of Co@C (yield = 65%). In addition, CoN_x@NC showed remarkable recyclability for six cycles with a minimum drop in the yield of the desired product.

Introduction

Amines play an important role as intermediates in the chemical industry and life sciences.[1] Their wide range of industrial applications include pharmaceuticals, organic dyes, agrochemicals, polymers, lubricants, and so on.[2] Additionally, the amine and nitrogen moieties play a key role in drug molecules.[3] Due to their high significance, numerous methods have been developed for the selective formation of C–N bonds.[1–4]

In general, secondary amines have been prepared by both oxidative and reductive methods.[5,6] In the reductive process, the carbonyl compound reacts with primary amines in the presence of a suitable catalyst and stoichiometric amounts of reducing agents (borohydride/formic acid/ammonium/formate/silanes).[7] This process generates a significant amount of waste and some of these are hazardous and difficult to handle.[7,8]

In the last few decades, oxidative catalytic approaches for C–N bond formation have been followed to enhance the activity and selectivity. One of the efficient catalytic oxidative approaches include *N*-alkylation of amines.[9] This process relies on hydrogen borrowing from the alcohol for the hydrogenation of imine, which is produced by the reaction of alcohol and primary amine.[10] As alcohols are abundant and only water is formed as the by-product, the method can be considered as an atom-economic and environmentally friendly approach.[10,11]

In recent years, *N*-alkylation reactions have successfully been carried out using homogenous noble metal complexes of Ru,[12,13] Ir,[2,14,15] Pd,[16] Au,[17] Pt,[18] *etc.*[19] These catalysts are highly effective for one-pot reactions. Although homogeneous catalysts show high efficiency, they have the typical drawbacks of limited recovery and reuse.[20,21] In addition, the use of expensive metals, ligands, and external additives makes the use of homogeneous catalysts impractical.[22] In this respect, heterogeneous noble metal catalysts of Pt,[23] Ru,[24,25] Pd,[26] Rh,[27] *etc.* have been used for *N*-alkylation of primary amines.[28] These catalysts also suffer from low selectivity, and the use of cocatalysts, high temperature and pressure, and high metal loading are required to improve the selectivity of *N*-alkylated products.[28]

On the other hand, transition metal-based heterogeneous catalysts have been demonstrated with promising catalytic activity for organic reactions.[29] Transition metal-based catalysts were found to produce high catalytic activity and selectivity for *N*-alkylation reactions.[30] As supported catalysts increase the surface area and provide more active sites for catalytic reactions, a series of solid-supported 3d transition metal-based catalysts were reported for the *N*-alkylation of amines.[31] For example, silica-supported Co,[32] Ni[33,34] and Cu[35,36] nanoparticles have been explored for the *N*-alkylation of amines. Other supports like metal oxides,[37,38] carbon,[39] *etc.* have been demonstrated for the immobilization of nanoparticles. The strong interaction between nanoparticles and the support is also important to stabilize nanoparticles on the support with minimum agglomeration during the catalytic process.[40,41]

Recently, nitrogen-doped carbon (NC) has been explored as a support material for heterogeneous catalysts due to its beneficial effect on tuning the chemical properties of catalysts.[42] NC-supported materials not only have high activity in

Department of Chemistry, Indian Institute of Technology (BHU), Varanasi, UP-221005, India. E-mail: arindam.chy@iitbhu.ac.in

† Electronic supplementary information (ESI) available: Syntheses and characterization of the catalysts, catalytic reactions and characterization of the products. See DOI: https://doi.org/10.1039/d3sc02515b

electrocatalysis, they also exhibit excellent catalytic properties for *N*-alkylation reactions.[29,30] For example, Beller and co-workers developed heterogeneous Co@NC for the *N*-alkylation of primary amines and ammonia.[43] Further, MN_x@NC catalysts were found to be highly efficient in catalytic organic transformations like *N*-alkylation of amines,[44] ester formation,[45] transfer hydrogenation,[46] hydrogenation,[47] *etc.* In this respect, the formation of M–N coordination was found to be useful to improve the catalyst–support interaction and hence enhance the stability of the system.[48]

The use of a metal–organic framework (MOF) having a N-containing bridging ligand as the precursor of MN_x@NC (M = transition metal, $x > 1$) has been explored by us and other groups.[49–51] The MOF helps in the uniform distribution of the metal nodes and provides the required coordination and electronic environment for the metal.[50] The pyrolysis of the MOF produces uniformly distributed nanoparticles on the surface of N-doped carbon, formed by the pyrolysis of the N-containing ligand.[52] The M–N coordination also stabilizes the nanoparticles on the N-doped carbon surface, which minimizes the particle agglomeration during the catalytic process and improves the stability of the catalyst.[42] The coordinated N to the metal center offers an environment, similar to the ligand in homogeneous catalysts, and manipulates the electron density on catalytic sites during the reaction.[42,50] Further, the adsorption of the substrate and reaction intermediates can also be modulated by the coordinated N. As a result, an improvement in the selectivity and catalytic activity can be achieved for organic transformations.[42,53,54]

Mostly, Co@NC,[49] Co–N–C,[55] and Fe–N–C[29] nanocatalysts with core–shell structures containing N-doped carbon (NC) shells have been reported for electrochemical energy conversion processes. The use of MOF-derived MN_x@NC nanocatalysts for organic transformations has been rarely studied.

Inspired by the above results, we report here the synthesis of a heterogeneous catalyst CoN_x@NC for the *N*-alkylation of amines. For this purpose, we have chosen ZIF-67@C as the precursor and pyrolyzed it to form CoN_x@NC. The ZIF-67 provides a unique coordination environment around the Co-center to form CoN_x@NC whereas the pyrolysis of the ligand produces N-doped graphene. The CoN_x@NC works as a hydrogen-borrowing catalyst for the alkylation of primary amines. The N-doped carbon supported CoN_x@NC showed excellent catalytic activity for *N*-alkylation reactions of amines with alcohols with the best yield of >99% for the desired product. Moreover, the catalyst was found to be stable enough during recycling for six catalytic cycles without having any significant drop in the catalytic activity and selectivity.

Results and discussion

Syntheses and characterization of the catalysts

The catalyst precursor ZIF-67@C was synthesized by the reaction of cobalt(II)nitrate and 2-methylimidazole in the presence of Vulcan-XC-72R carbon as the support (Scheme 1). The powder X-ray diffraction pattern (PXRD) of ZIF-67@C showed the characteristic crystal planes of ZIF-67 (JCPDS: 08-60-513,

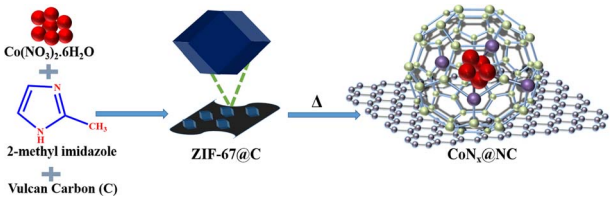

Scheme 1 The schematic representation for the synthesis of ZIF-67@C and its pyrolysis to produce CoN_x@NC.

Fig. S1†). The pyrolysis of ZIF-67@C in an inert atmosphere at different temperatures produced CoN_x@NCs (temperature = 700, 800, and 900 °C) (Scheme 1). The PXRD pattern of CoN_x@NC nanoparticles showed the face-centre cubic (fcc) crystal of cobalt (JCPDS: No.15-0806) (Fig. S2†).[48] In CoN_x@NC, the (111) peak of cubic cobalt was shifted towards the right side ($2\Theta = 0.3°$) due to the coordination with nitrogen (JCPDS: 08-60-513).

Further, the degree of graphitization of N-doped carbon (NC) in CoN_x@NC was investigated by Raman spectroscopy. The Raman spectrum showed the characteristic D and G bands of carbon at 1322 cm^{-1} and 1596 cm^{-1}, respectively (Fig. S3†).[56] The I_D/I_G ratio of 1.59 indicates a defect rich structure of NC. The classical E_g and A_{1g} vibronic modes of metallic Co were detected at 475 cm^{-1} and 682 cm^{-1}, respectively.

The nature of carbon was further analysed by X-ray photoelectron spectroscopy (XPS, Fig. 1). The C 1s XPS was fitted into five peaks for: sp^2 hybridised carbon of C=C (284.7 eV), sp^3 hybridised carbon C–C bond (284.9 eV), C=N (285.9 eV), C–N (287.6 eV), and COOH (290.1 eV).[57] The ratio of the graphitic carbon to other carbon is determined to be 1.62, which closely matches with the Raman data.

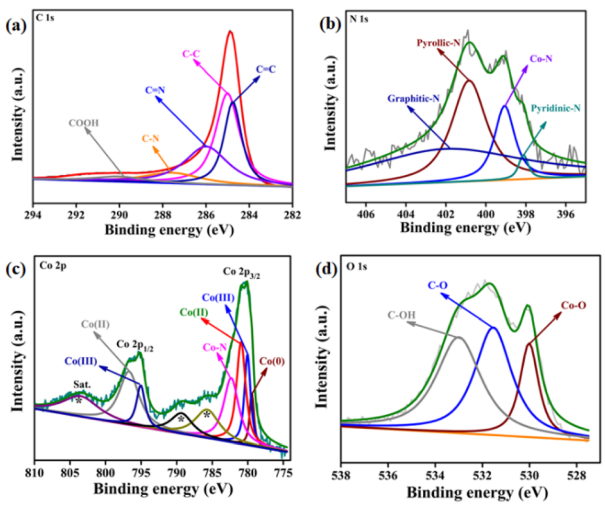

Fig. 1 (a) The C 1s spectrum of CoN_x@NC was deconvoluted into five peaks for C=C, C–C, C=N, C–N, and COOH species. (b) The N 1s spectrum was fitted into four peaks-corresponding to pyridinic, Co–N, pyrrolic, and graphitic nitrogen. (c) Co 2p XPS was fitted into peaks for Co(0), Co–N, Co(III), and Co(II) species. The * marked peaks originate as the satellite peaks of Co(II). (d) O 1s spectrum of CoN_x@NC.

The N 1s XPS was deconvoluted into four peaks at binding energies 398.1, 399.0, 400.8, and 401.7 eV corresponding to pyridinic, Co–N, pyrrolic, and graphitic nitrogen (Fig. 1b).[39] This result confirms the doping of N in the carbon matrix and the formation of the Co–N bond. Therefore, in the CoN_x@NC, the Co atoms are coordinated to the pyrolic-N and pyridinic-N and offer active sites during catalytic reactions.

The Co 2p XPS was fitted into two peaks corresponding to Co $2p_{3/2}$ (780.1 eV) and Co $2p_{1/2}$ (795.3 eV) (Fig. 1c).[55] The Co $2p_{3/2}$ peak was further deconvoluted into the peaks for Co^0 (779.3 eV) and Co–N (782.3 eV), Co(III) (779.9 eV), and Co(II) (780.8 eV) species. The presence of Co(III) and Co(II) species can be explained by the surface oxidation of cobalt nanoparticles. The O 1s XPS was deconvoluted into three peaks at 529.9, 531.5, and 533.0 eV corresponding to Co–O, C–O, and C–OH species (Fig. 1d).[58]

The scanning electron microscopy (SEM) images showed the rhombic dodecahedron morphology of CoN_x@NC where the Co nanoparticles of various sizes were densely embedded on NC (Fig. 2a and S4†). The energy dispersive X-ray (EDX) spectrum of CoN_x@NC revealed the presence of Co, N, and C (Fig. S5†) whereas the EDX elemental mapping showed the homogeneous distribution of Co on N-doped carbon (Fig. S6†).

Further, the morphological details of the catalyst were confirmed by transmission electron microscopy (TEM, Fig. 2b–d). The TEM images of CoN_x@NC demonstrated that the Co nanoparticles with varying sizes (4–12 nm) were distributed in the N-doped carbon frameworks (Fig. S7†). The selected area electron diffraction (SAED) pattern of CoN_x@NC showed diffraction rings corresponding to the crystal planes (111), (200), and (220) of fcc cobalt (Fig. 2d-inset). The inter-planar spacing of the N-doped carbon layer was calculated to be 0.36 nm, corresponding to the (002) plane of graphene (Fig. 2d).

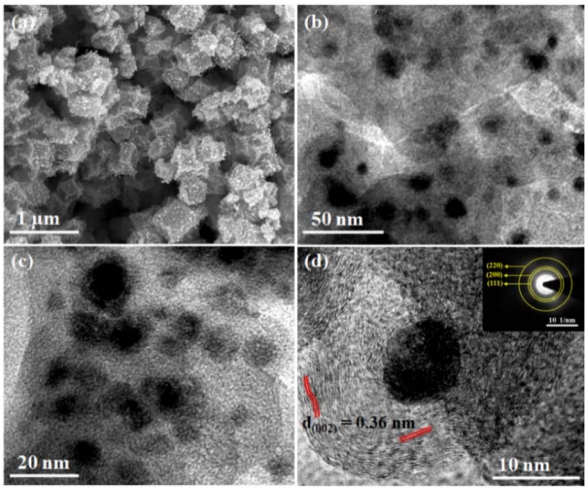

Fig. 2 (a) FE-SEM image of CoN_x@NC showing the rhombic dodecahedron morphology of the particles. (b and c) TEM images of CoN_x@NC with spherical morphology and the size of the particles was calculated to be 4–12 nm. (d) HR-TEM image showing the inter-planar spacing between the graphene layers and the inset shows the SAED pattern of the CoN_x@NC.

Optimization of the catalytic reaction conditions

First, the catalytic performance of CoN_x@NC was optimized for the *N*-alkylation reaction of benzyl alcohol and aniline (Table S1†). The reaction of benzyl alcohol with aniline can produce *N*-benzylaniline (**1**) and *N*-benzylideneaniline (**2**) as the major products. Therefore, control over the selectivity to produce **1** as the major product is a challenging task. The hydrogen borrowing route can be effectively employed to synthesize *N*-benzylaniline.

Interestingly, CoN_x@NC was found to be highly selective for the production of **1** when full conversion was achieved. For the comparison purpose, we used Co@C and found that the coordination of Co with N is extremely important for the improved selectivity and activity. While CoN_x@NC can produce **1** with 99% yield after the full conversion (entry 1, Table S1†), Co@C can reach the maximum yield of 65% (87% conversion) under the same reaction conditions (entry 4, Table S1†). The other catalysts had poor conversion and low selectivity for **1** (entries 5–7, Table S1†).

The pyrolysis temperature of the catalysts has also a significant effect on the conversion and selectivity of the products. Comparison of the catalysts prepared at different pyrolysis temperatures (700–900 °C) showed that CoN_x@NC (prepared at 800 °C) produced the best activity and selectivity for **1** (entries 1–3, Table S1†).

Further, the effect of different bases on the yield of **1** has been determined. The yield of **1** dropped in the absence of a base, and in the presence of bases, the yield of **1** followed the order: *tert*-BuOK > KOH > Cs_2CO_3 > K_2CO_3 (entries 8–12, Table S1†). The optimized amount of the CoN_x@NC catalyst was found to be 10 mg and poorer yield of **1** was obtained with lower (5 mg) or higher (15 mg) amount of catalyst (entries 13–15, Table S1†). Next, we optimized the effect of solvent and the best conversion and selectivity for **1** were recorded in toluene. Other non-polar aprotic solvents also produced high selectivity in the following order: toluene > THF > dioxane > acetonitrile (entries 16–19, Table S1†). In polar protic solvents like methanol and ethanol, we observed the formation of a mixture of products and we did not continue the reaction further.

Scope of different alcohols

With the optimized reaction conditions, the *N*-alkylation of aniline with different benzyl alcohols was studied (Scheme 2: **3a–3i** and Table S2†). In all the cases, secondary amines (**3**) were found to be the major product (yield = 81–99%). The best yield (99%) was obtained for the reaction of aniline with benzyl alcohol after 18 h of reaction (Scheme 2, **3a** and Table S2†). The methoxy-substitution at the *para*-position of benzyl alcohol slowed down the reaction but the yield of the secondary amine **3b** was not affected. However, a decrease in the yield of **3c** was observed when 2,4-dimethoxy-benzyl alcohol was reacted with aniline, most probably due to the increasing steric hindrance. On the other hand, the electron withdrawing substituent in the *meta*- and *para*-position of benzyl alcohol slightly decreases the yield of the corresponding secondary amines when reacted with aniline (Scheme 2, **3d–3f** and Table S2†).

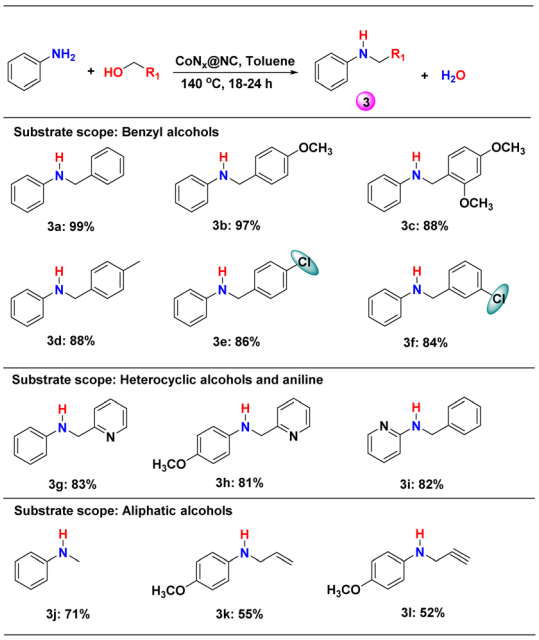

Scheme 2 *N*-alkylation of aniline and substituted-anilines with different benzyl alcohols using the CoN_x@NC catalyst. Reaction conditions: 1 mmol substituted benzyl alcohol, 0.5 mmol aniline, 10 mg catalyst, 0.5 mmol *tert*-BuOK, 2 mL toluene, 140 °C, 24 h. For 3a (18 h), 3e (18 h) and 3f (18 h) optimized at different times.

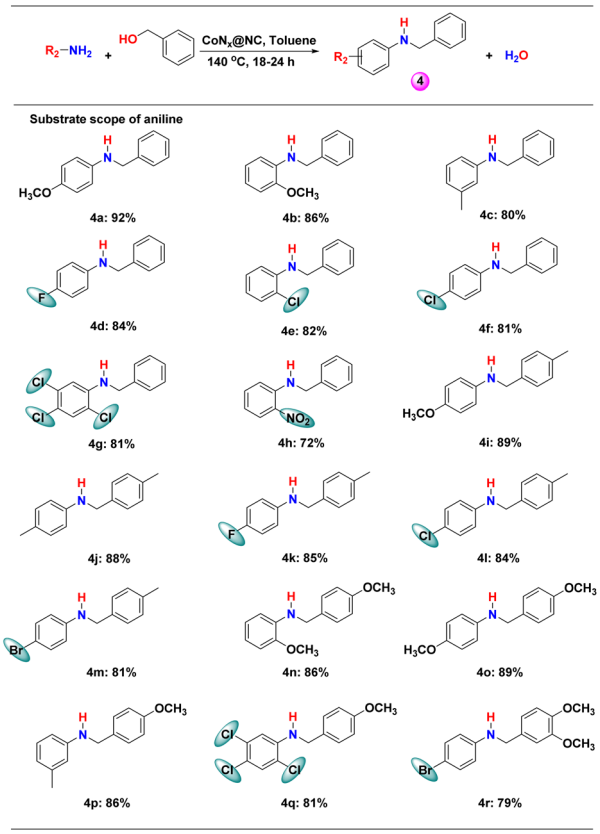

Scheme 3 CoN_x@NC catalysed *N*-alkylation reaction of different anilines with benzyl alcohols. Reaction conditions: 1 mmol substituted benzyl alcohol, 0.5 mmol aniline, 10 mg catalyst, 0.5 mmol *tert*-BuOK, 2 mL toluene, 140 °C, 24 h. For 4d (18 h), 4e (20 h) and 4f (20 h) optimized at different times.

The use of heterocyclic benzyl alcohol (pyridine-2-yl-methanol) decreased the yield of **3g** and **3h** (Scheme 2, Table S2†). Even, heterocyclic aniline with benzyl alcohol produced a high yield of secondary heterocyclic amines (Scheme 2, **3i**). The aliphatic alcohols were found to produce lower yield (52–71%) for *N*-alkylation than the benzylic alcohols (Scheme 2, **3j–3l** and Table S2†). The yield of the *N*-alkylated product decreased from methanol to propylene alcohol to propyne alcohol.

Scope of different anilines

Next, we explored the scope of different anilines for *N*-alkylation reactions with benzyl alcohol. Anilines with different electron donating and electron withdrawing substituents in the phenyl ring produced high yield (>80%) for secondary amines and the effect of the electronic factor on the product yield was not clear (Scheme 3 and Table S2†). However, a series of substituted anilines were selectively converted into secondary amines. The effect of steric crowding is distinct and the substitution in the *ortho*-position of anilines resulted in low yields (Scheme 3, **4b**, **4e**, **4g**, **4h**, **4n** and **4q**). The lowest yield (72%) among the studied substituted anilines was obtained with 2-nitroaniline due to the introduction of both steric crowding and electron-withdrawing effects (Scheme 3, **4h**).

When the steric crowding in both substrates was increased, a significant drop in the yield of the product was observed (Scheme 3, **4q** and **4r**). Therefore, CoN_x@NC is highly efficient in catalysing the *N*-alkylation of a series of anilines with different alcohols (benzyl alcohols, aliphatic primary alcohols, allylic alcohol, and alkyne alcohol).

Scope of *o*-phenylenediamine

As N-containing heterocyclic benzimidazole compounds are important components in anticancer, antibacterial, antitumor, anti-HIV and anthelmintic related drugs, we have explored the reaction of *o*-phenylenediamine with substituted benzyl alcohols to form benzimidazoles.[59] The reaction of *o*-phenylenediamine with benzyl alcohols having an electron donating and electron withdrawing group formed benzimidazoles with high yield (>78%) (**5a–c**, Scheme 4 and Table S2†).

To get an insight of the reaction pathway, the advancement of the reaction with time was monitored. The reaction of benzyl alcohol with aniline produced both *N*-benzylidene aniline (imine) and *N*-benzylaniline (secondary amine) (Fig. S8†). The time-dependent profile of the products clearly indicates that a consecutive reaction mechanism is followed for the formation of *N*-benzylaniline. Initially, the yield of the imine was high and it was converted to *N*-benzylaniline with time (Fig. S8†).

The hydrogen borrowing reaction mechanism was also established by a series of controlled reactions (Fig. S9†). According to the hydrogen borrowing methodology, the first step is the dehydrogenation of benzyl alcohol by [Co] to form benzaldehyde and H–[Co]–H (Scheme 5). We were able to detect 4-methoxy benzaldehyde as the major product when aniline was not introduced

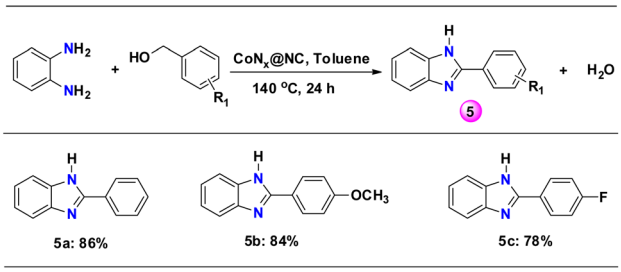

Scheme 4 *N*-alkylation reaction of *o*-phenylenediamine with substituted benzyl alcohols. Reaction conditions: 1 mmol substituted benzyl alcohol, 0.5 mmol *o*-phenylenediamine, 10 mg catalyst, 0.5 mmol Cs_2CO_3, 2 mL toluene, 140 °C, 24 h.

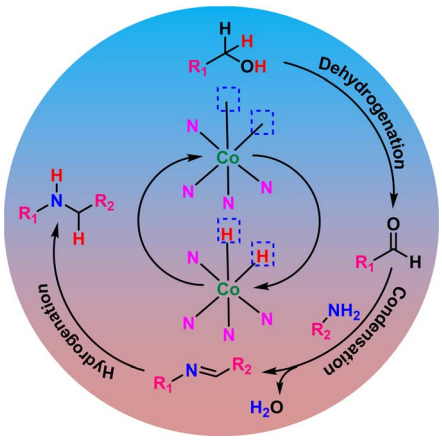

Scheme 5 Reaction mechanism for the *N*-alkylation reaction.

into the reaction mixture (Fig. S9†). Separately, the reaction of 4-methoxy benzaldehyde and 4-methoxyaniline in the presence of CoN_x@NC produced imine as the major product by the condensation process (Fig. S9†). The absence of the hydrogen borrowing process in the first step hindered the formation of H–[Co]–H and hence the production of secondary amine by the hydrogenation of imine was restricted (Fig. S9†). These reactions have clearly established that the first step is the dehydrogenation of benzyl alcohol to form benzaldehyde, which undergoes condensation with aniline to form imine, followed by the hydrogenation of imine to form secondary amine. The catalyst CoN_x@NC provides active sites for all three processes – dehydrogenation, condensation, and hydrogenation.

Recycling of the catalyst

We have investigated the recyclability of CoN_x@NC for the *N*-alkylation reaction of aniline and benzyl alcohol. After each reaction, the catalyst was separated from the reaction mixture by centrifugation and used for a new batch of reaction. The catalyst was recycled six times with a minor loss in the activity and yield (Fig. S10†).

Conclusions

In conclusion, MOF-derived CoN_x@NC catalysts have been developed for the *N*-alkylation of anilines with alcohols to produce secondary amines. In CoN_x@NC, the Co–N coordination, accessed through the pyrolysis of the MOF, was found to be beneficial to modulate the electron density on cobalt, optimize the binding of substrates and reaction intermediates on the catalyst surface and improve the yield of the desired product. The scope of a series of alcohols and anilines was explored and moderate to high yield of secondary amines was observed depending on substrates. Moreover, the catalyst has remarkable stability and versatile substrate scope for the synthesis of secondary amines.

Data availability

The data supporting this article have been uploaded as part of the ESI.†

Author contributions

VV synthesized and characterized the catalysts, carried out the catalytic reactions, interpreted the data and prepared the manuscript. PM was involved in the characterization of the catalysts. AI designed and conceptualized the project and edited the manuscript.

Conflicts of interest

There are no conflicts of interest.

Acknowledgements

This work is financially supported by CSIR [01(2977)/19/EMR-II], Govt. of India. VV thanks CSIR for providing the senior research fellowship.

Notes and references

1 S. Elangovan, J. Neumann, J. B. Sortais, K. Junge, C. Darcel and M. Beller, *Nat. Commun.*, 2016, **7**, 1–8.
2 Y. Wang, F. L. Zhang, Z. J. Liu and Z. J. Yao, *Inorg. Chem.*, 2022, **61**, 10310–10320.
3 S. Chakraborty, R. Mondal, S. Pal, A. K. Guin, L. Roy and N. D. Paul, *J. Org. Chem.*, 2023, **88**, 771–787.
4 J. Bariwal and E. Van Der Eycken, *Chem. Soc. Rev.*, 2013, **42**, 9283–9303.
5 J. I. Ramsden, R. S. Heath, S. R. Derrington, S. L. Montgomery, J. Mangas-Sanchez, K. R. Mulholland and N. J. Turner, *J. Am. Chem. Soc.*, 2019, **141**, 1201–1206.
6 C. Zhang, Q. Liang, W. Yang, G. Zhang, M. Hu and G. Zhang, *Green Chem.*, 2022, **24**, 7368–7375.
7 K. Murugesan, T. Senthamarai, V. G. Chandrashekhar, K. Natte, P. C. J. Kamer, M. Beller and R. V. Jagadeesh, *Chem. Soc. Rev.*, 2020, **49**, 6273–6328.
8 E. Pedrajas, I. Sorribes, K. Junge, M. Beller and R. Llusar, *Green Chem.*, 2017, **19**, 3764–3768.
9 P. Ruiz-Castillo and S. L. Buchwald, *Chem. Rev.*, 2016, **116**, 12564–12649.

10 B. G. Reed-Berendt, D. E. Latham, M. B. Dambatta and L. C. Morrill, *ACS Cent. Sci.*, 2021, **7**, 570–585.
11 T. Irrgang and R. Kempe, *Chem. Rev.*, 2019, **119**, 2524–2549.
12 M. H. S. A. Hamid, C. L. Allen, G. W. Lamb, A. C. Maxwell, H. C. Maytum, A. J. A. Watson and J. M. J. Williams, *J. Am. Chem. Soc.*, 2009, **131**, 1766–1774.
13 J. J. A. Celaje, X. Zhang, F. Zhang, L. Kam, J. R. Herron and T. J. Williams, *ACS Catal.*, 2017, **7**, 1136–1142.
14 O. Saidi, A. J. Blacker, M. M. Farah, S. P. Marsden and J. M. J. Williams, *Chem. Commun.*, 2010, **46**, 1541–1543.
15 I. Borthakur, M. Maji, A. Joshi and S. Kundu, *J. Org. Chem.*, 2022, **87**, 628–643.
16 T. T. Dang, B. Ramalingam, S. P. Shan and A. M. Seayad, *ACS Catal.*, 2013, **3**, 2536–2540.
17 M. Stratakis and H. Garcia, *Chem. Rev.*, 2012, **112**, 4469–4506.
18 T. Ohshima, Y. Miyamoto, J. Ipposhi, Y. Nakahara, M. Utsunomiya and K. Mashima, *J. Am. Chem. Soc.*, 2009, **131**, 14317–14328.
19 A. Corma, J. Navas and M. J. Sabater, *Chem. Rev.*, 2018, **118**, 1410–1459.
20 A. Indra, M. Greiner, A. K. Gericke, R. Schlögl, D. Avnir and M. Driess, *ChemCatChem*, 2014, **6**, 1935–1939.
21 B. Goel, V. Vyas, N. Tripathi, A. Kumar Singh, P. W. Menezes, A. Indra and S. K. Jain, *ChemCatChem*, 2020, **12**, 5743–5749.
22 S. Rojas-Buzo, P. Concepción, A. Corma, M. Moliner and M. Boronat, *ACS Catal.*, 2021, **11**, 8049–8061.
23 C. Chaudhari, S. M. A. H. Siddiki, K. Kon, A. Tomita, Y. Tai and K. I. Shimizu, *Catal. Sci. Technol.*, 2014, **4**, 1064–1069.
24 R. Cano, D. J. Ramón and M. Yus, *J. Org. Chem.*, 2011, **76**, 5547–5557.
25 L. Wang, X. Jv, R. Wang, L. Ma, J. Liu, J. Sun, T. Shi, L. Zhao, X. Zhang and B. Wang, *ACS Sustain. Chem. Eng.*, 2022, **10**, 8342–8349.
26 V. Goyal, J. Gahtori, A. Narani, P. Gupta, A. Bordoloi and K. Natte, *J. Org. Chem.*, 2019, **84**, 15389–15398.
27 P. Tomkins, C. Valgaeren, K. Adriaensen, T. Cuypers and D. E. D. Vos, *ChemCatChem*, 2018, **10**, 3689–3693.
28 E. Podyacheva, O. I. Afanasyev, D. V. Vasilyev and D. Chusov, *ACS Catal.*, 2022, **12**, 7142–7198.
29 W. Liu, L. Zhang, X. Liu, X. Liu, X. Yang, S. Miao, W. Wang, A. Wang and T. Zhang, *J. Am. Chem. Soc.*, 2017, **139**, 10790–10798.
30 P. Y. Wu, G. P. Lu and C. Cai, *Green Chem.*, 2021, **23**, 396–404.
31 V. Goyal, N. Sarki, A. Narani, G. Naik, K. Natte and R. V. Jagadeesh, *Coord. Chem. Rev.*, 2023, **474**, 214827.
32 V. G. Chandrashekhar, K. Natte, A. M. Alenad, A. S. Alshammari, C. Kreyenschulte and R. V. Jagadeesh, *ChemCatChem*, 2022, **14**, e202101234.
33 K. I. Shimizu, N. Imaiida, K. Kon, S. M. A. Hakim Siddiki and A. Satsuma, *ACS Catal.*, 2013, **3**, 998–1005.
34 A. Afanasenko, S. Elangovan, M. C. A. Stuart, G. Bonura, F. Frusteri and K. Barta, *Catal. Sci. Technol.*, 2018, **8**, 5498–5505.
35 H. Liu, G. K. Chuah and S. Jaenicke, *J. Catal.*, 2015, **329**, 262–268.
36 M. Dixit, M. Mishra, P. A. Joshi and D. O. Shah, *Catal. Commun.*, 2013, **33**, 80–83.
37 K. Natte, H. Neumann, R. V. Jagadeesh and M. Beller, *Nat. Commun.*, 2017, **8**, 1–9.
38 F. Kallmeier, R. Fertig, T. Irrgang and R. Kempe, *Angew. Chem., Int. Ed.*, 2020, **59**, 11789–11793.
39 C. Li, Y. Meng, S. Yang and H. Li, *ChemCatChem*, 2021, **13**, 5166–5177.
40 S. Rösler, M. Ertl, T. Irrgang and R. Kempe, *Angew. Chem., Int. Ed.*, 2015, **54**, 15046–15050.
41 A. Tomer, F. Wyrwalski, C. Przybylski, J. F. Paul, E. Monflier, M. Pera-Titus and A. Ponchel, *J. Catal.*, 2017, **356**, 111–124.
42 A. Indra, T. Song and U. Paik, *Adv. Mater.*, 2018, **30**, 1–25.
43 Z. Ma, B. Zhou, X. Li, R. G. Kadam, M. B. Gawande, M. Petr, R. Zbořil, M. Beller and R. V. Jagadeesh, *Chem. Sci.*, 2022, **13**, 111–117.
44 F. Kallmeier, R. Fertig, T. Irrgang and R. Kempe, *Angew. Chem., Int. Ed.*, 2020, **59**, 11789–11793.
45 H. Su, K. X. Zhang, B. Zhang, H. H. Wang, Q. Y. Yu, X. H. Li, M. Antonietti and J. S. Chen, *J. Am. Chem. Soc.*, 2017, **139**, 811–818.
46 Z. An and J. Li, *Green Chem.*, 2022, **24**, 1780–1808.
47 J. Gao, R. Ma, L. Feng, Y. Liu, R. Jackstell, R. V. Jagadeesh and M. Beller, *Angew. Chem., Int. Ed.*, 2021, **60**, 18591–18598.
48 X. Liu, L. Xu, G. Xu, W. Jia, Y. Ma and Y. Zhang, *ACS Catal.*, 2016, **6**, 7611–7620.
49 H. Guo, Q. Feng, J. Zhu, J. Xu, Q. Li, S. Liu, K. Xu, C. Zhang and T. Liu, *J. Mater. Chem. A*, 2019, **7**, 3664–3672.
50 B. Singh and A. Indra, *Mater. Today Energy*, 2020, **16**, 100404.
51 J. Li, B. Wang, Y. Qin, Q. Tao and L. Chen, *Catal. Sci. Technol.*, 2019, **9**, 3726–3734.
52 H. Konnerth, B. M. Matsagar, S. S. Chen, M. H. G. Prechtl, F. Shieh and K. C. Wu, *Coord. Chem. Rev.*, 2020, **416**, 213319.
53 G. Li, H. Yang, H. Zhang, Z. Qi, M. Chen, W. Hu, L. Tian, R. Nie and W. Huang, *ACS Catal.*, 2018, **8**, 8396–8405.
54 R. V. Jagadeesh, K. Murugesan, A. S. Alshammari, H. Neumann, M. M. Pohl, J. Radnik and M. Beller, *Science*, 2017, **358**, 326–332.
55 A. K. Singh, S. Ji, B. Singh, C. Das, H. Choi, P. W. Menezes and A. Indra, *Mater. Today Chem.*, 2022, **23**, 100668.
56 Y. Xue, N. N. T. Pham, G. Nam, J. Choi, Y. Y. Ahn, H. Lee, J. Jung, S. G. Lee and J. Lee, *Chem. Eng. J.*, 2021, **408**, 127305.
57 Z. Lin, G. Waller, Y. Liu, M. Liu and C. P. Wong, *Adv. Energy Mater.*, 2012, **2**, 884–888.
58 C. Yuan, J. Li, L. Hou, X. Zhang, L. Shen and X. W. Lou, *Adv. Funct. Mater.*, 2012, **22**, 4592–4597.
59 K. Chakrabarti, M. Maji and S. Kundu, *Green Chem.*, 2019, **21**, 1999–2004.